

Supplementary Information - Supervised learning in a mechanical system

Menachem Stern, Chukwunonso Arinze, Leron Perez, Stephanie Palmer, Arvind Murugan

Physics Department and the James Franck Institute,

University of Chicago, Chicago, IL 60637

Supplementary Note 1 - Folding origami sheets

Energy of folded structures

The origami sheets used in this work are based on a self-folding origami energy model developed and validated in previous studies [1–3]. The effects of stiff creases are modeled by using torsional spring elements on each crease [4, 5]. Here we discuss in detail how the energy of a folded structure is computed.

For thin origami sheets with free-folding creases, the primary contribution to the energy of a folded structure is due to bending of the sheet faces. Instead of modelling the faces directly, we look at the mechanical constraints inherent to the geometry of the vertices. An origami vertex is known to apply 3 constraints on the dihedral folding angles of the creases connected to it (due to embedding of the sheet in 3d-space). The constraints can be derived by noting that the vertex must not tear open when folded. Thus, starting from any crease, alternating rotations about the dihedral and sector angles around the vertex have to result in an identity operation [2, 4, 5].

Suppose there are N creases denoted by an index i , each folded to an angle ρ_i , and N sectors with angles θ_i around the vertex. Rotations about one dihedral angle and one sector would combine to form a rotation matrix

$$R_i = \begin{pmatrix} 1 & 0 & 0 \\ 0 & \cos \rho_i & -\sin \rho_i \\ 0 & \sin \rho_i & \cos \rho_i \end{pmatrix} \begin{pmatrix} \cos \theta_i & -\sin \theta_i & 0 \\ \sin \theta_i & \cos \theta_i & 0 \\ 0 & 0 & 1 \end{pmatrix}. \quad (1)$$

For the vertex to be closed (i.e. not torn open) in a folded structure, the combination of rotation about all crease dihedral angles and sector angles must be the identity:

$$A \equiv \prod_{i=1}^n R_i = I. \quad (2)$$

A folded structure with values ρ_i that do not satisfy Eq. 2 must cause the sheet faces to bend. Mathematically, this effect will manifest in finite off-diagonal values in the matrix $A \equiv \prod_{i=1}^N R_i$. As there are 3 independent non-diagonal elements, we say that the vertex imparts 3 mechanical constraints on the dihedral angles ρ_i around it.

of external torques \mathbf{F}^{ext} is given (this could be a training or a test example as described in the main text). First, the sheet is folded very fast with a strong external torque \mathbf{F}^{ext} , until a certain folding magnitude $\rho \equiv \|\boldsymbol{\rho}\|$ is reached. For fast folding we can initially disregard the sheet energy and thus get to a state

$$\boldsymbol{\rho}_{\text{fast}} = \rho \frac{\mathbf{F}^{ext}}{\|\mathbf{F}^{ext}\|}.$$

Then the sheet is relaxed subject to the constraint that the overall folding magnitude is fixed (i.e. finding an energy minimum on a hyper-sphere of radius ρ in ρ -space):

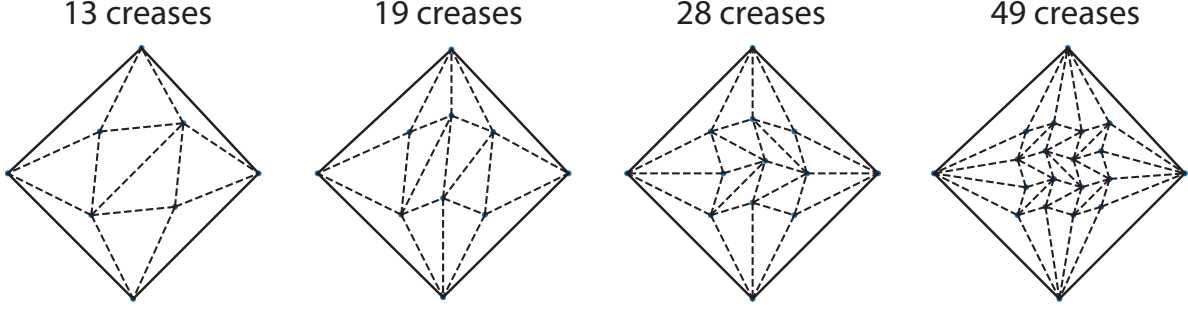
$$\begin{aligned} & \underset{\rho_i}{\text{minimize}} && E_{\text{sheet}}(\boldsymbol{\rho}) \\ & \text{subject to} && \|\boldsymbol{\rho}\| = \rho. \end{aligned} \tag{6}$$

Finding a local minimum on the hyper-sphere guarantees that this folded structure would naturally occur if the sheet is folded with appropriate torques, as any neighboring configuration costs more energy, and the local minimum will attract the folding process. This algorithm is used to mimic experimental fast folding of origami sheets, followed by clamping of a crease at a specific folded dihedral angle. Here we also adjust the clamped angle such that the overall magnitude of folding ρ remains fixed and different (discrete) folded structures may be compared more easily. Such fast folding was tested extensively [5], and found to obtain the same results as numerically solving the ODE of Eq. 5.

Origami sheets and applied force patterns

In this project we use specific self-folding origami sheets. These are triangulated thin sheets, chosen to have the property of self-foldability. As discussed above, a single vertex induces 3 mechanical constraints on the angles of creases surrounding it. Thus each vertex has to connect at least 4 creases or it would be locally rigid. On top of that, for a sheet to self-fold, it needs to have one global degree of freedom, so that the number of creases needs to be one more than the number of constraints.

A simple way of generating patterns meeting these requirements is shown in Supplementary Fig. 1. These are 4 specific geometries used throughout this work as the sheets to be trained. Note that we label them according to their size, given by the number creases



Supplementary Figure 1. Origami Sheets used for training. The size of each sheet is determined by the number creases.

in each sheet. The number of creases in these sheets are 13, 19, 28, 49 and the numbers of internal vertices are 4, 6, 9, 16. Subtracting 3 times the number of vertices from the number of creases leaves us with one global degree of freedom for each of these sheets, as required.

The number of supported folded structures for these sheets grows exponentially with the number of internal vertices, such that these sheets can fold in approximately $2^4, 2^6, 2^9, 2^{16}$ distinct ways [4, 7]. In fact, any sheet with these topologies (yet different geometries) will have a similar number of distinct folded structures. The exact details of the supported folded structures is dependent on the specific geometry, but we only require the existence of many distinct folded structures for the purpose of training.

These specific sheets, used for training classifiers throughout this work, are definitely not special. We attempted training classifiers using sheets with different geometries and obtained comparable results. In analogy to learning algorithms, the details of the sheet and its supported folded structures correspond to the family of models that the training protocol selects from. For origami, we believe the available classification models are given by merger of attractors of folded structures, supported by the sheet. Since the number of available models to choose from is exponentially large, we reason that the geometry of the sheet should play little role in the success of classification. Therefore, any self-folding origami sheet could be used for training classifiers.

The choice of force patterns applied to the sheets is constrained by the problem definition as training and tests sets. Still, there is usually freedom in how these forces are applied. For example, suppose we wish to train the 13 crease sheet of Supplementary Fig. 1 on $2d$ force distributions, such as the spherical caps shown in Fig. 3 in the main text. The training and

test sets could thus be supplied as pairs of numbers, together with a label (blue\orange). A simple choice for training on such a data set is to pick two creases in the sheet and apply torques directly to these creases, as in Eq. (5). Here we utilize a different approach.

For an untrained sheet with homogeneous stiffness, it is known that all folded structures reside in the linear null space of the vertex constraint matrix C at the flat state [4]. Thus, forces applied in a direction within this null space are more ‘natural’ for the sheet, and in general cost much less energy due to face bending. We compute the span of the null space for each one of these sheets, and find that the dimension of the null space is $d_{NS} = \#_{\text{creases}} - 2\#_{\text{vertices}}$. Therefore the 13 crease sheet has a $5d$ null space, while the 49 crease sheets has $17d$ null space. Then, the training and test examples are mapped to forces in the null space as follows. For a $n - d$ data set, we choose n random orthonormal vectors in the null space. Each training\test example is mapped to a force pattern by assigning every component to one of the random orthonormal vectors. Now these forces can be directly applied to the sheet to facilitate the training protocol.

Training results in heterogeneous crease stiffness values that change the geometry of the folded structures, so that they do not strictly reside in the null space of the untrained sheet. Still, for the moderate heterogeneity developed during training, the observed folded structures are very close to the null space, such that the described mapping is still useful and practical.

Supplementary Note 2 - Training origami sheets

Learning rule

As discussed in the main text, self-folding origami sheets naturally give rise to complex mapping of force patterns to folded structures, with exponentially many structures supported by the sheet. The learning rule developed in this work is meant to modify that map by changing crease stiffness coefficients, such that only a small number of folded structures are retained, corresponding to the desired classes. Here we will define precisely how the learning rule is chosen and applied to the sheet in order to develop the desired mapping.

According to the specification of the classification problem, the trainer has no a-priori

knowledge of the true underlying force distributions. Instead they are supplied with a list of labeled force patterns (‘cats’ and ‘dogs’). These training examples are used to find a reference folded structure in the following way. We fold an untrained sheet with every ‘dog’ example in the training set and record the folding angles of the obtained folded structures. Then, a reference ‘dog’ structure $\hat{\boldsymbol{\rho}}_{\text{dog}}$ is defined as the average of all of these folded structures (normalized appropriately)

$$\hat{\boldsymbol{\rho}}_{\text{dog}} \equiv \frac{\sum_{\mathbf{F} \in \mathcal{F}^{\text{dog}}} \boldsymbol{\rho}_U(\mathbf{F})}{\|\sum_{\mathbf{F} \in \mathcal{F}^{\text{dog}}} \boldsymbol{\rho}_U(\mathbf{F})\|}, \quad (7)$$

with \mathcal{F}^{dog} the set of ‘dog’ training force patterns and $\boldsymbol{\rho}_U(\mathbf{F})$ the folded response of the untrained sheet to force pattern \mathbf{F} . A similar reference state $\hat{\boldsymbol{\rho}}_{\text{cat}}$ is obtained for the ‘cat’ training examples. Crucially, once the reference structures are set for the untrained sheet, they are kept fixed throughout the training process. These reference structures are used to define the learning rule discussed in the main text. Suppose that during the training protocol, we choose a random ‘dog’ example \mathbf{F}^{dog} and apply it to the sheet. The normalized resulting folded structure is written as $\boldsymbol{\rho}(\mathbf{F}^{\text{dog}})$. The learning rule then compares this folded structure to the reference structures defined above and the stiffness coefficients are modified as follows:

$$\begin{aligned} \text{if } \boldsymbol{\rho}(\mathbf{F}^{\text{dog}}) \cdot \hat{\boldsymbol{\rho}}_{\text{dog}} > \boldsymbol{\rho}(\mathbf{F}^{\text{dog}}) \cdot \hat{\boldsymbol{\rho}}_{\text{cat}} : & \quad \frac{dk_i}{dt} = -\alpha \rho_i^2(\mathbf{F}^{\text{dog}}) \\ \text{else :} & \quad \frac{dk_i}{dt} = +\alpha \rho_i^2(\mathbf{F}^{\text{dog}}). \end{aligned} \quad (8)$$

$k_i \geq 0, i \in \text{creases}$

In essence, the learning rule checks whether the observed folded structure is closer to the ‘dog’ reference than to the ‘cat’ reference. If it does, the stiffness of creases that fold considerably in that structure is reduced, effectively reinforcing this force-fold mapping. An opposite modification occurs if the folded structure is far away from the ‘dog’ reference. A similar training rule is used when ‘cat’ forces patterns are applied, with the understanding that we wish to compare the resulting folded structure $\boldsymbol{\rho}(\mathbf{F}^{\text{cat}})$ to the ‘cat’ reference $\hat{\boldsymbol{\rho}}_{\text{cat}}$.

Assigning labels to folded structures

To begin with, we are given labeled force patterns, and an untrained sheet with many available folded structures. It is important to note that these folded structures are equivalent and not intrinsically labeled. Thus, as part of the learning protocol we must specify how to label these folded structures, and in particular which of them to call ‘dog’ and ‘cat’ (or ‘blue’ and ‘orange’). A simple solution would be to choose 2 of the folded structures in advance and assign the classification labels to them. Unfortunately, this turns out to be too restrictive for a couple of reasons. First, the choice may be far from ideal in the sense that these labeled folded structures are very different than the actual folded response of the sheet to the labeled force patterns. Furthermore, as the training process modifies the stiffness of different creases, the folded structures supported by the sheet change as well, either by moving around or disappearing altogether in saddle-node bifurcations [5]. We thus take a different approach to labeling folded structures, as detailed below.

Suppose we have trained a sheet for some time, and it now has a particular stiffness profile on its creases k_i . To find a folded structure of this sheet to be labeled ‘dog’, we apply each of the ‘dog’ training examples once, and record the discrete resulting folded structures due to all of them $\{\rho(\mathbf{F} \in \mathcal{F}^{\text{dog}})\}$. We then count the training force patterns that folded into each one of the structures in this set. The folded structure that resulted from the largest number of training force patterns is chosen to be labeled as ‘dog’. In case of a tie, e.g. two or more folded structures folding as a result of the same number of force patterns, one of these structures is randomly chosen to serve as the label. Thus, the labels for ‘dog’ and ‘cat’ are decided through simple plurality rules every time we compute the classification accuracy of the sheet. Note that force patterns may also fold the sheet into structures not labeled as either ‘cat’ or ‘dog’, in which case they count as failed classification. If both ‘dog’ and ‘cat’ labels are chosen to be associated with the same folded structure, a plurality rule between the two classes decides which class is labeled with that structure (i.e. whether more ‘cat’ or ‘dog’ force patterns folded into that structure), while the other is assigned with the runner up structure of that labels’ plurality vote. Finally, if the sheet is over-trained to the point where only one folded structure remains, that structure is labeled as both ‘cat’ and ‘dog’, such that classification fails completely, by definition.

Effective cost function

In this work we have defined our learning rule as a supervised physical process modifying the stiffness coefficients of an origami sheet. It is interesting to compare this kind of learning protocol to more established learning algorithms originating in computer science and statistics. One important difference is that traditional learning algorithms are usually defined as an optimization problem, where the function to be optimized (often called cost or loss function) incorporates the training data.

A simple example is linear regression, where the cost function is usually chosen as a least squares form, where the differences are taken between a linear model $h(x)$ and the observations y :

$$\begin{aligned} \text{Cost} &\equiv \sum_{d \in \text{data}} (h(x_d) - y_d)^2 \\ h(x) &= a_0 + a_1 x \end{aligned} \tag{9}$$

The regression (or learning algorithm) then optimizes the cost function with respect to the model parameters $\mathbf{a} \equiv (a_0, a_1)$

$$\underset{\mathbf{a}}{\text{minimize}} \quad \text{Cost}(\{x\}, \{y\}; \mathbf{a}).$$

This optimization can be achieved in any number of ways, but a practically favored method (at least for more advanced algorithms like deep learning) is mini-batch stochastic gradient descent (SGD) [8]. In an extreme case, when the mini-batches are chosen to be of size 1, a single training example (x, y) is chosen at random in each step, and one computes the gradient (with respect to parameters \mathbf{a}) of the cost function defined with this example alone $\mathbf{G} \equiv \nabla_{\mathbf{a}}(h(x) - y)^2$. Now, training proceeds by modifying the parameters in proportion to the the gradient of this single example cost function

$$\mathbf{a} \rightarrow \mathbf{a} - \alpha \mathbf{G}, \tag{10}$$

where α is a scalar known as the learning rate. We may compare this single example SGD with our origami training protocol. It is relatively easy to see that our training rule (Eq. 8), once a standard wait time is chosen at the folded state, has the form of SGD, making it

similar in essence to other learning algorithms. To find out what effective cost function gives rise to the origami learning rule, we integrate Eq. 8 with respect to the stiffness coefficients

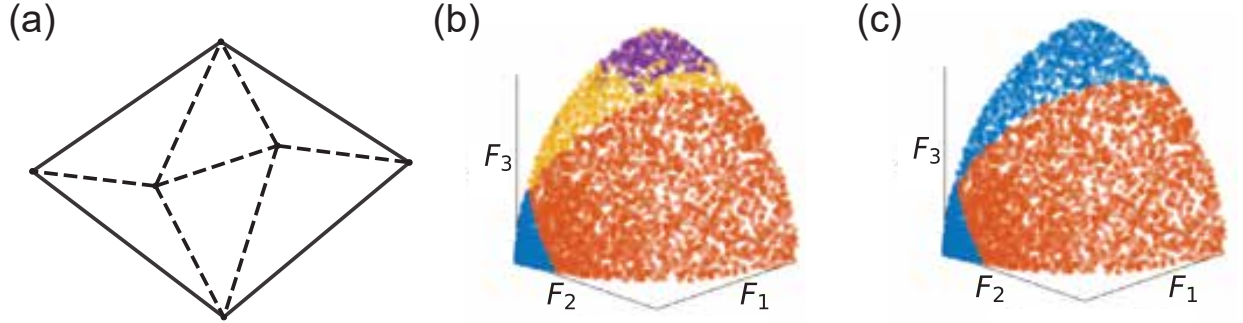
$$\begin{aligned} \text{cost}_{\text{map}}(\boldsymbol{\rho}(\mathbf{F}^{\text{dog}})) &= f \sum_{i \in \text{creases}} k_i \rho_i^2(\mathbf{F}^{\text{dog}}) \\ \text{if } \boldsymbol{\rho}(\mathbf{F}^{\text{dog}}) \cdot \hat{\boldsymbol{\rho}}_{\text{dog}} &> \boldsymbol{\rho}(\mathbf{F}^{\text{dog}}) \cdot \hat{\boldsymbol{\rho}}_{\text{cat}} : & f = +1 \quad . \\ \text{else :} & & f = -1 \end{aligned} \tag{11}$$

Similarly to the linear regression example, our origami training protocol attempts to minimize this derived cost function, one training example at a time. Inspecting this function, note that it is very similar to the energy of the torsional springs in the folded structure $E_{\text{Crease}}(\boldsymbol{\rho}) \sim \sum_i k_i \rho_i^2$. The difference is in the ‘supervising factor’ f that can be ± 1 whether the folded structure is accepted or not. We conclude that our origami training protocol is attempting to minimize the energy of accepted folded structures, while maximizing the energy of rejected structures.

Supplementary Note 3 - Using origami sheets to define classification problems

The force distributions classified in the main text are relatively simple. Both the spherical cap and the Iris data distributions can be well separated by a hyper-plane, a very simple decision boundary. It is interesting to study the type of decision boundaries naturally trainable in origami sheets – and whether they can be used to classify intrinsically high dimensional data.

There are many ways to obtain high dimensional distributions. Here we choose to study distributions derived from the folding maps of origami sheets. Consider a relatively simple sheet with 2 internal vertices (Supplementary Fig. 2a). It is known that such sheets support 4 discrete folded structures, and that the linearized null space in which they reside is 3-dimensional. Therefore, if we sample random force patterns within this null space, we expect to see the sheet folding into 4 distinct structures (color coded regions in Supplementary Fig. 2b). The forces F_1, F_2, F_3 are assigned by randomly choosing Euler angles on the 2-sphere, and 3000 data points are sampled on the positive octant. Note that we sample



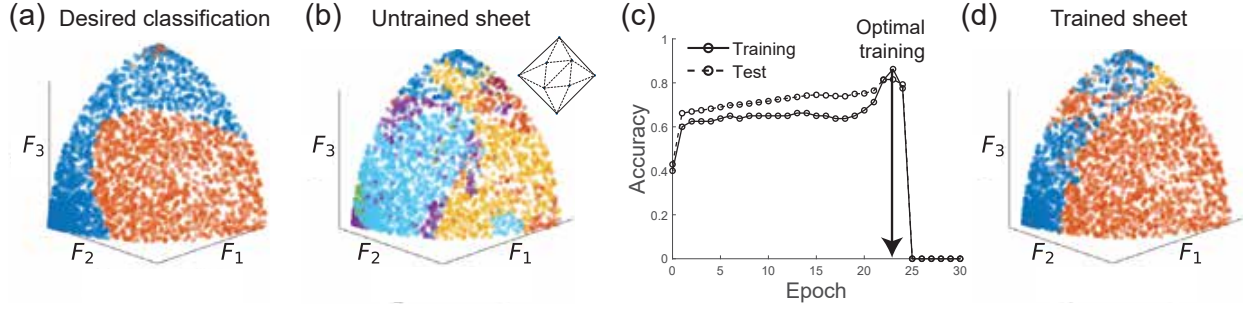
Supplementary Figure 2. Defining force distributions using the force-fold mapping of an origami sheet. a) Origami sheets with 2 internal vertices support 4 discrete folded structures. b) Sample force patterns on a 2-sphere show the force-fold mapping (4 color coded regions). c) When some attractor regions are merged (here, blue, yellow and purple are merged), we obtain an intrinsically 2-dimensional separator surface between two classes of force patterns.

normalized forces on the surface of a 2-sphere, such that the distribution of force patterns is actually 2-dimensional.

Now, suppose we wish to classify forces to 2 classes ('blue'\ 'orange'). A simple way to create 2 neighboring sets of points is to take the data of Supplementary Fig. 2b and merge some attractor regions to create larger groups of points. In Supplementary Fig. 2c, we merge the 'blue', 'yellow', and 'purple' folded structures to create one region we define as 'blue'. This process yields two distributions that are intrinsically 2-dimensional, and not naturally separable by a hyper-plane. Larger sheets can be similarly used to create force distributions in higher dimensional space.

With this process, we have access to a new variety of 2-way classification problems, on which we can try to train origami sheets using the training protocol described in the main text. Crucially, the sheet used to classify such distributions is different than the sheet used to derive the distribution. In other words, we ask if our training protocol can induce an origami sheet to mimic the force-fold mapping of another sheet.

Suppose we want to classify the distribution seen in Supplementary Fig. 3a, derived from a 2-vertex sheet as described above. We wish to train a 13 crease sheet to classify this force pattern data. The untrained sheet has 2^4 discrete folded structures that do not align with the target distribution in any representation that we tested (Supplementary Fig. 3b). The



Supplementary Figure 3. Training a sheet on a force distribution derived from a different sheet. a) Target classification, a sample distribution derived from a small, 2-vertex origami sheet. b) The force-fold map of an untrained 13 crease sheet is very different from the desired mapping. c) With training, the accuracy of classification improves and peaks at 82%. d) The optimally trained sheet has a complex decision boundary that resembles (but different than) the desired boundary.

problem of classification here is to train this sheet to have just 2 folded structures with the right force-fold mapping as in the target distribution.

The target distribution is mapped to applied force patterns on the 13 crease sheet by the construction describe in Supplementary Note 1: choosing random orthonormal vectors in the null space of the 13 crease sheet and mapping the distribution as components of these vectors. We then randomly sample 20 ‘blue’ and 20 ‘orange’ force patterns, marked as diamonds in Supplementary Fig. 3, to serve as the training set. As we train the sheet, the classification accuracy improves dramatically and reaches a maximum of 82% (test accuracy) after 23 epochs (Supplementary Fig. 3c). To qualify the classification better, we look at the classification results corresponding to the maximal accuracy at epoch 23 (Supplementary Fig. 3d). We observe that the trained decision boundary resembles the desired boundary, so that the training protocol indeed produced a reasonable classification.

Note a few artifacts that still remain in the trained map: 1) there are 3 folded structures left, rather than 2 (a small third color coded region exists, labeled yellow), 2) a second orange region appeared inside the bulk blue region, emphasizing that the decision boundaries between folded structures in sheets are generally *not* hyper-planes. We conclude that origami sheets can be trained to classify distributions derived from other sheets, that are intrinsically higher dimensional than the problems discussed in the main text. We leave questions of the sheet size and the complexity of decision boundaries to future studies.

Supplementary Note 4 - Transforming Iris data to applied forces on sheets

The Iris data set [9] classified in the main text is a classical problem for classification. In this work we are able to train an origami sheet to correctly classify two species of Iris (I. Versicolor, I. Virginica) at an accuracy of 91%. Here we discuss how the Iris data is used to generate training and test sets of applied force patterns to be used on origami sheets.

Each Iris example in the data set is given as a vector with 4 features (components): sepal length, sepal width, petal length, petal width. These length measurements are all given in *cm*. In addition to these measurements, each Iris is labeled as one of the Iris species in the study. To generate force pattern sets from this data, we would like the different measurements for each Iris example to be components of force vectors in the null space of the origami sheet, as described in Supplementary Note 1. However, the raw Iris data is not suited for this purpose due to two reasons. The dimensional measurements of Iris lengths, if directly translated to forces, would be far too great for our sheets and will cause it to fold too much and cause the sheet faces to collide. More crucially, sepal and petal lengths tend to be considerably larger than their widths, and the same goes for the variance of these variables. This will cause the width variables to be perceived as less important in the training protocol, and have a negative effect on the classification results.

Fortunately, diverse data like this is an issue regularly faced by learning algorithms, and it is generically solved by applying an invertible transformation to the data. The transformed data is then better suited for the learning algorithm in use. A typical example of such a transformation in data sets is to normalize each feature (divide by the mean of that feature) and translate it such that the mean of the transformed data is 0. This transformation is especially useful for classification algorithms like logistic regression, where the different features have different dimensional units.

In our case however, the standard transformation above is not useful, due to a particular property of origami sheets, namely their Z_2 symmetry. If forces \mathbf{F} are applied to the sheet and it folds into a state $\boldsymbol{\rho}$, then folding the same sheet with forces $-\mathbf{F}$ will result in a state $-\boldsymbol{\rho}$. This is true for any self-folding origami sheet, regardless of the stiffness profile on its creases. This property cannot be changed by training the sheet. Thus, force patterns of

opposite sign and different labels cannot be correctly classified. A simple way to avoid this issue is to limit the force patterns to reside in a restricted part of force space. We choose to limit the distributions such that the transformed Iris data will all be in the positive 4-hyperoctant.

In addition, we want the data to span as much as possible of the positive hyperoctant. This will increase the expressive of our training protocol, as more discrete folded structures would become available if the applied force patterns are more diverse. We thus need to transform the Iris data to be all positive, and stretch it such that all features have similar variance.

To achieve these goals we apply the following linear (invertible) transformation to the Iris data of the Versicolor and Virginica species. Suppose an Iris example is given as a vector \mathbf{x} (where the components are sepal length, sepal width, petal length, petal width in this order). The vector is transformed by

$$\mathbf{x}^* = A\mathbf{x} + b$$

$$A = \begin{pmatrix} 0.264 & 0 & 0 & 0 \\ 0 & 0.580 & 0 & 0 \\ 0 & 0 & 0.303 & 0 \\ 0 & 0 & 0 & 0.836 \end{pmatrix}, \quad b = -0.880. \quad (12)$$

Then the transformed vector is used to define the force patterns applied to the origami sheet, as described in Supplementary Note 1. After training is concluded, the transformation can be inverted to relate the origami classification results with the original Iris data, as shown in the main text.

-
- [1] Sarah-Marie Belcastro and Thomas C Hull. Modelling the folding of paper into three dimensions using affine transformations. *Linear Algebra and its applications*, 348(1):273–282, 2002.
 - [2] Tomohiro Tachi. Geometric considerations for the design of rigid origami structures. In *Proceedings of the International Association for Shell and Spatial Structures (IASS) Symposium*, volume 12, pages 458–460, 2010.
 - [3] Matthew B Pinson, Menachem Stern, Alexandra Carruthers Ferrero, Thomas A Witten, Eliz-

- abeth Chen, and Arvind Murugan. Self-folding origami at any energy scale. *Nat. Commun.*, 8:15477, 18 May 2017.
- [4] Menachem Stern, Matthew B Pinson, and Arvind Murugan. The complexity of folding self-folding origami. *Phys. Rev. X*, 7(4):041070, 2017.
 - [5] Menachem Stern, Viraa Jayaram, and Arvind Murugan. Shaping the topology of folding pathways in mechanical systems. *Nat. Commun.*, 9(1):4303, 2018.
 - [6] Edwin A Peraza-Hernandez, Darren J Hartl, Richard J Malak Jr, and Dimitris C Lagoudas. Origami-inspired active structures: a synthesis and review. *Smart Materials and Structures*, 23(9):094001, 2014.
 - [7] Bryan Gin-ge Chen and Christian D Santangelo. Branches of triangulated origami near the unfolded state. *Physical Review X*, 8(1):011034, 2018.
 - [8] Sebastian Ruder. An overview of gradient descent optimization algorithms. *arXiv preprint arXiv:1609.04747*, 2016.
 - [9] Ronald A Fisher. The use of multiple measurements in taxonomic problems. *Annals of eugenics*, 7(2):179–188, 1936.